1-1-1992

Charge Storage In The Quasi-Neutral Regions Of Si Homojunction, Algaas/Gaas Heterojunction, And Si/Sige Heterojunction Bipolar-Transistors

J. J. Liou
University of Central Florida

Charge storage in the quasineutral regions of Si homojunction, AlGaAs/GaAs heterojunction, and Si/SiGe heterojunction bipolar transistors

Cite as: Journal of Applied Physics **71**, 4059 (1992); https://doi.org/10.1063/1.350830
Submitted: 06 September 1991 . Accepted: 14 January 1992 . Published Online: 17 August 1998

J. J. Liou

Charge storage in the quasineutral regions of Si homojunction, AlGaAs/GaAs heterojunction, and Si/SiGe heterojunction bipolar transistors

J. J. Liou
Electrical Engineering Department, University of Central Florida, Orlando, Florida 32816

(Received 6 September 1991; accepted for publication 14 January 1992)

Charge storage in the quasineutral regions of a bipolar transistor often limits the switching speed of the device, particularly when the transistor is operated in saturation mode (both emitter-base and base-collector junctions are forward biased), a bias condition which occurs frequently in logic circuits. This paper studies and compares the free-carrier charges stored in the quasineutral regions of the conventional Si homojunction bipolar transistor (Si BJT) and the increasingly important AlGaAs/GaAs and Si/SiGe heterojunction bipolar transistors (HBTs). The diffusion capacitances associated with this stored charge, which are used in the Gummel–Poon bipolar transistor model, are also calculated and discussed. It is shown that the AlGaAs/GaAs HBT has the least carrier accumulation in the quasineutral regions among the three devices due primarily to the relatively large energy band gap of GaAs-related materials. Also, the Si/SiGe HBT is expected to operate at a higher switching speed compared to the Si BJT, because the valence band discontinuity at the Si/SiGe base-collector heteroface impedes the minority-carrier injection from the base into the collector.

I. INTRODUCTION

Operation speed of a bipolar junction transistor (BJT) is limited by removing and injecting the free-carrier charges stored in the junction space-charge regions and in the quasineutral regions. The charge storage in the quasineutral regions is usually more prominent, particularly when the emitter-base and base-collector junctions are forward biased (saturation operation), as is often the case for logic circuits. At thermal equilibrium, no current is allowed to flow because the drift and diffusion tendencies are equal and in opposite directions in the space-charge layer. The balance is destroyed when a forward voltage is applied to the junction, which reduces the drift tendency from its equilibrium value. Consequently, the minority carriers are injected into the opposite sides of the junction because the diffusion tendency is stronger than the drift tendency in the space-charge layer. Once reaching the quasineutral region, these minority carriers are governed only by the diffusion tendency and diffuse toward the other end of the quasineutral region. In steady state, these traveling charges are considered stored in the quasineutral region. When the minority-carrier transit time across the quasineutral region is much longer compared to the change of the excitation in transient condition, the switching speed of the bipolar transistor is limited by the time required to supply or remove these charges.

The recent advances in epitaxy technology, i.e., molecular-beam epitaxy (MBE) and metalorganic chemical vapor deposition (MOCVD), has made it possible to grow high-quality heterojunctions. In contrast to a homojunction, which yields the same barrier heights for the electron and hole fluxes across the junction, the heterojunction can provide unequal barrier heights for electron and hole, thus impeding one of the free-carrier fluxes across the junction. Such an heterojunction can be implemented in the heterojunction bipolar transistor (HBT) to reduce the base current and increase the current gain; the heterostructure pair for the emitter and base of the HBT can be selected such that the heterojunction causes an extra barrier for minority-carrier injection from the base into the emitter. Many HBTs have been actively investigated for high-speed digital and microwave applications, but AlGaAs/GaAs and Si/SiGe HBTs have received the most attention and are perhaps the most promising devices.[1,2] In an AlGaAs/GaAs HBT, the energy band gap in the emitter is increased by adding Al into GaAs. In a Si/SiGe HBT, however, the energy band gap in the base is reduced by adding Ge into Si. Either case results in a heterojunction formed by the wider-band-gap emitter and the narrower-band-gap base. The popularity of AlGaAs/GaAs HBTs stems from the high electron mobility of GaAs and the close lattice constants of AlGaAs and GaAs. Si/SiGe HBTs possess the advantages of being compatible with existing and well-established Si technology as well as having very low bulk and surface electron-hole recombination, which maintains a high current gain at low collector current regime. Because the substrates are GaAs and Si for AlGaAs/GaAs and Si/SiGe HBTs, respectively, an AlGaAs/GaAs/GaAs single HBT (emitter-base heterojunction and base-collector homojunction) and a Si/SiGe/Si double HBT (emitter-base and base-collector heterojunctions) come about naturally.[3]

This paper investigates the minority-carrier charge storage in the quasineutral regions of the conventional Si BJT and the increasingly important AlGaAs/GaAs and Si/SiGe HBTs. Analytical models are developed to calculate the charge storage and their relevant capacitances, and the results for the three different devices are compared. This study should provide a quick estimate on the free-carrier charge stored in each quasineutral region and fur-

 0021-8979/92/084059-07$04.00

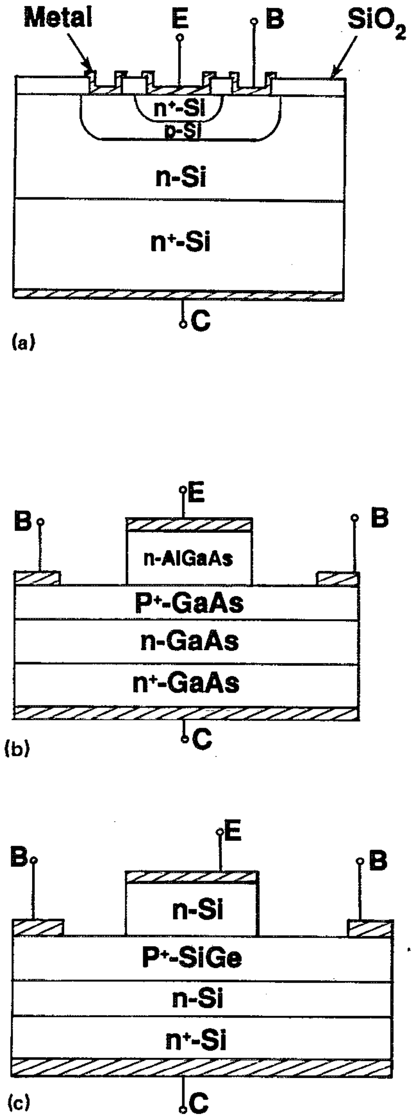

FIG. 1. The device structure of (a) Si homojunction BJT; (b) AlGaAs/GaAs HBT; and (c) Si/SiGe HBT.

nish useful physical insights into the switching speed of the Si BJT, AlGaAs/GaAs HBT, and Si/SiGe HBT limited by this charge storage.

II. THEORETICAL DEVELOPMENT

Figures 1(a)–1(c) show the device structures of *n/p/n* Si/Si/Si BJT, AlGaAs/GaAs/GaAs single HBT (SHBT), and Si/SiGe/Si double HBT (DHBT). The theoretical development will focus on the DHBT, since the SHBT and BJT are just special cases of the DHBT. In circuit simulations, the incremental change in the minority-carrier charge stored in the quasineutral regions with respect to the change in the voltage can be represented by the emitter-base diffusion capacitance C_{DE} and the base-collector diffusion capacitance C_{DC},[4] as shown in the widely used Gummel–Poon bipolar transistor model given in Fig. 2. The former results from the minority-carrier injection

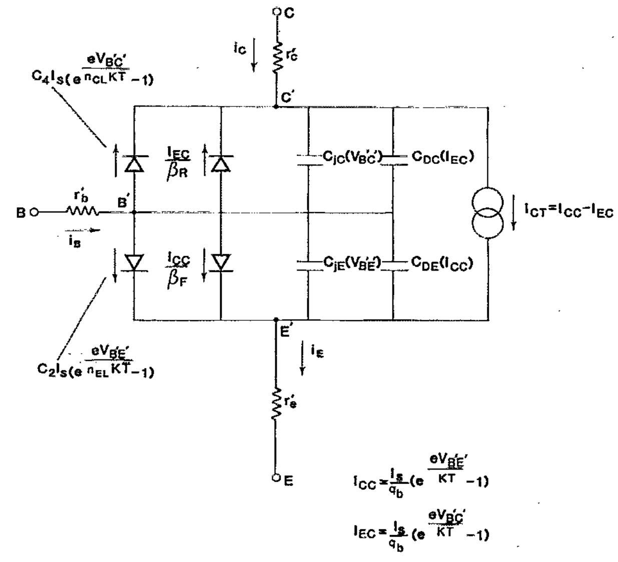

FIG. 2. Circuit representation of the Gummel–Poon bipolar transistor model, where C_{DE} and D_{DC} are the diffusion capacitances result from the charge storage in the quasineutral regions, and C_{jE} and C_{jC} are the junction capacitances result from the charge storage in the space-charge regions.

across the forward-biased emitter-base junction, and the latter is due to the minority-carrier injection across the forward base-collector junction. Note that C_{DC} is zero if the transistor is operated in forward-active mode (emitter-base junction forward biased and base-collector junction reverse biased). Figure 3 shows the energy band diagram of the DHBT, indicating the conduction band and valence band discontinuities at the emitter-base heteroface ($\Delta E_{C,EB}$ and $\Delta E_{V,EB}$), the conduction band and valence band discontinuities at the base-collector heteroface ($\Delta E_{C,BC}$ and $\Delta E_{V,BC}$), the quasineutral emitter (QNE), the quasineutral base (QNB), the quasineutral collector (QNC), the emitter-base space-charge region (EB SCR), and the base-collector space-charge region

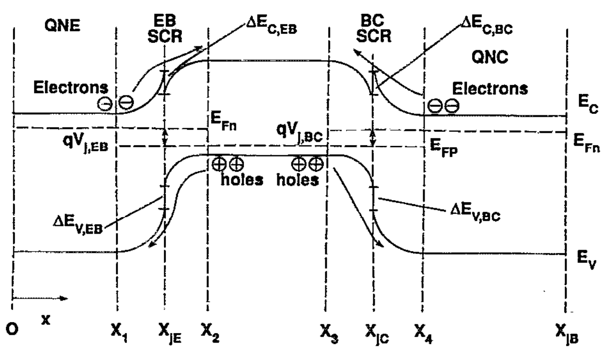

FIG. 3. Energy band diagram of the double HBT in saturation operation (both the emitter-base and the base-collector junctions are forward biased). In the figure, X_{jE}, X_{jC}, and X_{jB} are the metallurgical junctions and X_1 X_2, X_3, and X_4 are the edges of the space-charge layers. E_{Fn} and E_{Fp} represent the electron and hole quasi-Fermi energy levels, which are separated by $qV_{j,BE}$ in the emitter-base space-charge layer and by $qV_{j,BC}$ in the base-collector space-charge layer, respectively.

(BC SCR). For the DHBT under study, $\Delta E_{C,\mathrm{EB}} = \Delta E_{C,\mathrm{BC}} \equiv \Delta E_C$ and $\Delta E_{V,\mathrm{EB}} = \Delta E_{V,\mathrm{BC}} \equiv \Delta E_V$.

A. Charge storage associated with emitter-base junction

The emitter-base diffusion capacitance is given by

$$C_{\mathrm{DE}} = C_{\mathrm{QNE}} + C'_{\mathrm{QNB}}. \tag{1}$$

C_{QNE} and C'_{QNB} are the QNE and QNB diffusion capacitances result from the forward-biased emitter-base junction

$$C_{\mathrm{QNE}} = dQ_{\mathrm{QNE}}/dV_{\mathrm{BE}} \quad \text{and} \quad C'_{\mathrm{QNB}} = dQ'_{\mathrm{QNB}}/dV_{\mathrm{BE}}, \tag{2}$$

where V_{BE} is the base-emitter applied voltage and Q_{QNE} and Q'_{QNB} are the minority-carrier charges stored in the QNE and QNB due to the forward-biased emitter-base junction, respectively. Assume short emitter and short base, as is often the case in advanced bipolar transistors. Then the excess minority-carrier concentrations (Δn and Δp) distribute linearly in the QNE and QNB. Thus

$$Q_{\mathrm{QNE}} = q \int_0^{X_1} p(x)dx \approx q\left(\frac{n_{\mathrm{iE}}^2 X_1}{N_E} + 0.5\Delta p(X_1)X_1\right), \tag{3}$$

$$Q'_{\mathrm{QNB}} = q \int_{X_2}^{X_3} n(x)dx \approx q\left(\frac{n_{\mathrm{iB}}^2(X_3 - X_2)}{N_B} + 0.5\Delta n(X_2)(X_3 - X_2)\right), \tag{4}$$

where n_{iE} and n_{iB} are effective intrinsic free-carrier concentrations in the emitter and base, respectively, including the heavy doping effect,[5] X_1 and X_2 are the edges of the emitter-base space-charge layer (Fig. 3), X_3 is the edge of the base-collector space-charge layer in the base region (Fig. 3), N_E is the emitter-doping concentration, and N_B is the base doping concentration. Using the drift-diffusion concept, assuming that the quasi-Fermi levels are flat throughout the space-charge layer, and taking into account the energy band discontinuities, the excess free-carrier concentrations at the edges of the space-charge layer are given by[6]

$$\Delta p(X_1) \approx N_B \exp[-(V_{\mathrm{bi,EB}} - V_{j,\mathrm{BE}} + \Delta E_V/q)/V_T] - n_{\mathrm{iE}}^2/N_E, \tag{5}$$

$$\Delta n(X_2) \approx N_E \exp[-(V_{\mathrm{bi,EB}} - V_{j,\mathrm{BE}} - \Delta E_C/q)/V_T] - n_{\mathrm{iB}}^2/N_B. \tag{6}$$

$V_{\mathrm{bi,EB}}$ is the emitter-base junction built-in voltage and $V_{j,\mathrm{BE}}$ is the voltage drop across the base-emitter space-charge layer (or the emitter-base junction voltage) (Fig. 3),

$$V_{j,\mathrm{BE}} = V_{\mathrm{BE}} - V_{r,\mathrm{QNE}} - V_{r,\mathrm{QNB}}. \tag{7}$$

$V_{r,\mathrm{QNE}}$ and $V_{r,\mathrm{QNB}}$ are the voltage drops in the QNE and QNB, respectively. Since the doping concentrations in the emitter and base are high, $V_{j,\mathrm{BE}} \approx V_{\mathrm{BE}}$. Also, X_1 and X_2 depend weakly on V_{BE} [X_1 and X_2 are proportional to $(V_{\mathrm{BE}})^{0.5}$ according to the depletion approximation], they can be assumed independent of V_{BE}. This yields

$$C_{\mathrm{QNE}} = 0.5qX_1[d\Delta p(X_1)/dV_{\mathrm{BE}}] = 0.5qX_1N_B \exp[-(V_{\mathrm{bi,EB}} - V_{\mathrm{BE}} + \Delta E_V/q)/V_T]/V_T, \tag{8}$$

$$C'_{\mathrm{QNB}} = 0.5q(X_3 - X_2)[d\Delta n(X_2)/dV_{\mathrm{BE}}] = 0.5q(X_3 - X_2)N_E \exp[-(V_{\mathrm{bi,EB}} - V_{\mathrm{BE}} - \Delta E_C/q)/V_T]/V_T. \tag{9}$$

The above equations need modifications when high-level injection prevails. Let V'_{BE} and V''_{BE} be the onset base-emitter voltages for high-level injection in the emitter [$\Delta p(X_1) \approx p(X_1) \approx n(X_1) \approx N_E$ when $V_{\mathrm{BE}} = V'_{\mathrm{BE}}$] and in the base [$\Delta n(X_2) \approx n(X_2) \approx p(X_2) \approx N_B$ when $V_{\mathrm{BE}} = V''_{\mathrm{BE}}$], respectively. Thus

$$V'_{\mathrm{BE}} = V_T \ln[(n_{\mathrm{iE}}^2/N_E + N_E)/N_B] + V_{\mathrm{bi,EB}} + \Delta E_V/q, \tag{10}$$

$$V''_{\mathrm{BE}} = V_T \ln[(n_{\mathrm{iB}}^2/N_B + N_B)/N_E] - V_{\mathrm{bi,EB}} + \Delta E_C/q. \tag{11}$$

Since the free-carrier concentration in high injection follows the $\exp(V_{\mathrm{BE}}/2V_T)$ relation,[7] we have

$$\Delta p(X_1) \approx N_E \exp[(V_{\mathrm{BE}} - V'_{\mathrm{BE}})/2V_T] \quad \text{for} \quad V_{\mathrm{BE}} > V'_{\mathrm{BE}}, \tag{12}$$

$$\Delta n(X_2) \approx N_B \exp[(V_{\mathrm{BE}} - V''_{\mathrm{BE}})/2V_T] \quad \text{for} \quad V_{\mathrm{BE}} > V''_{\mathrm{BE}}. \tag{13}$$

The diffusion capacitances in high-level injection are given by

$$C_{\mathrm{QNE}} = 0.5qX_1N_E \exp[(V_{\mathrm{BE}} - V'_{\mathrm{BE}})/2V_T]/2V_T \quad \text{for} \quad V_{\mathrm{BE}} > V'_{\mathrm{BE}}, \tag{14}$$

$$C'_{\mathrm{QNB}} = 0.5q(X_3 - X_2)N_B \exp[(V_{\mathrm{BE}} - V''_{\mathrm{BE}})/2V_T]/2V_T \quad \text{for} \quad V_{\mathrm{BE}} > V''_{\mathrm{BE}}. \tag{15}$$

B. Charge storage associated with the base-collector junction

The base-collector diffusion capacitance can be expressed as

$$C_{\mathrm{DC}} = C_{\mathrm{QNC}} + C''_{\mathrm{QNB}}, \tag{16}$$

and

$$C_{\mathrm{QNC}} = dQ_{\mathrm{QNC}}/dV_{\mathrm{BC}}, \tag{17}$$

$$C''_{\mathrm{QNB}} = dQ''_{\mathrm{QNB}}/dV_{\mathrm{BC}}, \tag{18}$$

where V_{BC} is the base-collector applied voltage ($V_{\mathrm{BC}} > 0$ if base-collector forward biased), C_{QNC} and C''_{QNB} are the QNC and QNB diffusion capacitances due to the forward-biased base-collector junction, respectively, and Q_{QNC} and Q_{QNB} are the minority-carrier charge storage in the QNC and QNB, respectively. Again, assuming that the excess minority carrier distributes linearly in the QNB and QNC, we have

$$Q_{\rm QNC}=q[n_{\rm iC}^2(X_{\rm jB}-X_4)/N_C+0.5\Delta p(X_4)(X_{\rm jB}-X_4)], \tag{19}$$

$$Q''_{\rm QNB}=q[n_{\rm iB}^2(X_3-X_2)/N_B+0.5\Delta n(X_3)(X_3-X_2)]. \tag{20}$$

$n_{\rm iC}$ is the intrinsic free-carrier concentration in the collector, N_C is the collector doping concentration, and $X_{\rm jB}$ and X_4 are defined in Fig. 3. The excess free-carrier concentrations at the edges of the base-collector space-charge layer are[6]

$$\Delta p(X_4)\approx N_B\exp[-(V_{\rm bi,BC}-V_{j,\rm BC}+\Delta E_V/q)/V_T] - n_{\rm iC}^2/N_C, \tag{21}$$

$$\Delta n(X_3)\approx N_C\exp[-V_{\rm bi,BC}-V_{j,\rm BC}-\Delta E_C/q)/V_T] - n_{\rm iB}^2/N_B. \tag{22}$$

$V_{\rm bi,BC}$ is the base-collector junction built-in potential, and $V_{j,\rm BC}$ is the voltage drop across the base-collector space-charge layer (or the base-collector junction voltage) (Fig. 3)

$$V_{j,\rm BC}=V_{\rm BC}-V_{r,\rm QNB}-V_{r,\rm QNC}\approx V_{\rm BC}-V_{r,\rm QNC}, \tag{23}$$

where $V_{r,\rm QNC}$ is the voltage drop in the QNC which is not negligible because the collector doping concentration is low. $V_{r,\rm QNC}$ can be approximated as[8]

$$V_{r,\rm QNC}\approx J_C(X_{\rm jB}-X_4)/qN_C\mu_n, \tag{24}$$

where μ_n is the electron mobility and J_c is the collector-terminal current density[8]

$$J_C\approx q\mu_nV_T[\Delta n(X_2)-\Delta n(X_3)]/(X_3-X_2). \tag{25}$$

A simple iteration scheme is needed to calculate J_C, $V_{r,\rm QBC}$, and $V_{j,\rm BC}$ for a given $V_{\rm BC}$.

The QNC and QNB diffusion capacitances can be derived from the above equations as

$$C_{\rm QNC}=0.5q(X_{\rm jB}-X_4)[d\Delta p(X_4)/dV_{j,\rm BC}] = 0.5q(X_{\rm jB}-X_4)N_B\exp[-V_{\rm bi,BC}-V_{j,\rm BC} + \Delta E_V/q)/V_T]/V_T, \tag{26}$$

$$C''_{\rm QNB}=0.5q(X_3-X_2)[d\Delta p(X_3)/dV_{j,\rm BC}] = 0.5q(X_3-X_2)N_C\exp[-(V_{\rm bi,BC}-V_{j,\rm BC} - \Delta E_C/q)/V_T]/V_T. \tag{27}$$

The total charge $Q_{\rm QNB}$ stored in the QNB is $Q'_{\rm QNB}+Q''_{\rm QNB}$.

In high-level injection condition,

$$\Delta p(X_4)\approx N_C\exp[(V_{j,\rm BC} - V'_{\rm BC})/2V_T] \quad \text{for} \quad V_{j,\rm BC}>V'_{\rm BC}, \tag{28}$$

$$\Delta n(X_3)\approx N_B\exp[(V_{j,\rm BC} - V''_{\rm BC})/2V_T] \quad \text{for} \quad V_{j,\rm BC}>V''_{\rm BC}, \tag{29}$$

TABLE I. Device parameters used in calculation.

	Si BJT	$Al_{0.3}Ga_{0.7}As$/GaAs SHBT	$Si/Si_{0.7}Ge_{0.3}$ DHBT
$\Delta E_{C,\rm EB}$(eV)	0	0.21	0.02
$\Delta E_{V,\rm EB}$(eV)	0	0.19	0.25
$\Delta E_{C,\rm BC}$(eV)	0	0	0.02
$\Delta E_{V,\rm BC}$(eV)	0	0	0.25
N_E(cm^{-3})	10^{19}	10^{18}	10^{18}
N_B(cm^{-3})	10^{18}	10^{19}	10^{19}
N_C(cm^{-3})	5×10^{16}	5×10^{16}	5×10^{16}
$X_{\rm jE}$(μm)	0.2	0.1	0.1
$X_{\rm jC}$(μm)	0.6	0.2	0.2
$X_{\rm jB}$(μm)	1.2	0.7	0.7
$n_{\rm iE}$(cm^{-3})	1.5×10^{10}	10^4	1.5×10^{10}
$n_{\rm iB}$(cm^{-3})	1.5×10^{10}	1.8×10^6	7.0×10^{11}
$n_{\rm iC}$(cm^{-3})	1.5×10^{10}	1.8×10^6	1.5×10^{10}

and

$$C_{\rm QNC}=0.5q(X_{\rm jB}-X_4)N_C\exp[(V_{j,\rm BC} - V'_{\rm BC})/2V_T]/2V_T \quad \text{for} \quad V_{\rm BC}>V'_{\rm BE}, \tag{30}$$

$$C''_{\rm QNB}=0.5q(X_3-X_2)N_B\exp[(V_{j,\rm BC} - V''_{\rm BC})/2V_T]/2V_T \quad \text{for} \quad V_{\rm BC}>V''_{\rm BE}, \tag{31}$$

where $V'_{\rm BC}$ and $V''_{\rm BC}$ are the onset base-collector junction voltages for high-level injection in the collector and in the base, respectively,

$$V'_{\rm BC}=V_T\ln[(n_{\rm iC}^2/N_C+N_C)/N_B]+V_{\rm bi,BC}+\Delta E_V/q, \tag{32}$$

$$V''_{\rm BC}=V_T\ln[(n_{\rm iB}^2/N_B+N_B)/N_C]+V_{\rm bi,BC}-\Delta E_C/q. \tag{33}$$

III. DEVICE PARAMETERS

Device parameters used in calculations for typical Si BJT, AlGaAs/GaAs SHBT, and Si/SiGe DHBT are given in Table I. There are several key differences among the three devices. First, because of the valence band discontinuity which impedes hole injection from the base to emitter (Fig. 3), the HBTs can have a higher base doping concentration than the homojunction BJT while still maintaining a high current gain. Second, the homojunction BJT has a thicker base than the HBTs, necessitated by the prevention of punch through in the base, because of the relatively low base doping concentration. Third, the emitter of the AlGaAs/GaAs HBT is usually made of $Al_{0.3}Ga_{0.7}As$, an alloy composition that provides the widest energy band gap without altering significantly the physical properties of GaAs such as the three-valley direct band-gap energy band diagram. Fourth, the material of the base of the Si/SiGe HBT is selected so as to make the SiGe band gap about 0.25 eV smaller than that of Si,[9] which requires a strained $Si_{0.7}Ge_{0.3}$ alloy layer.[3] The values of the band discontinuities for the AlGaAs/GaAs and Si/SiGe heterojunctions (Table I) are obtained from that reported by Unlu and Nussbaum[10] and by King *et al.*,[3] respectively.

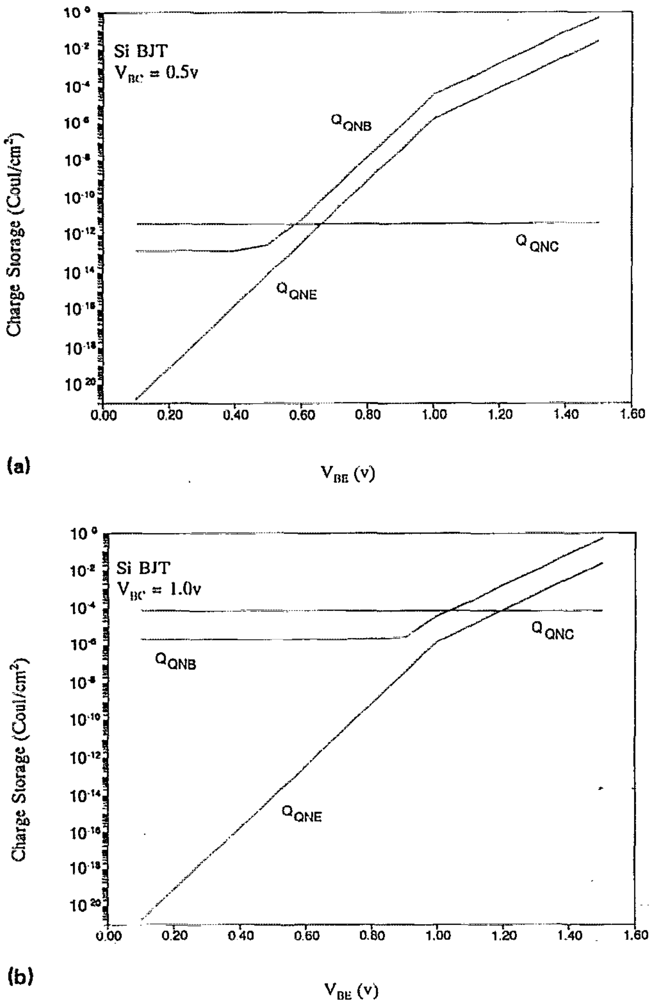

FIG. 4. Charge storage in the quasineutral emitter, base, and collector of the Si homojunction BJT for (a) $V_{BC}=0.5$ V; and (b) $V_{BC}=1.0$ V.

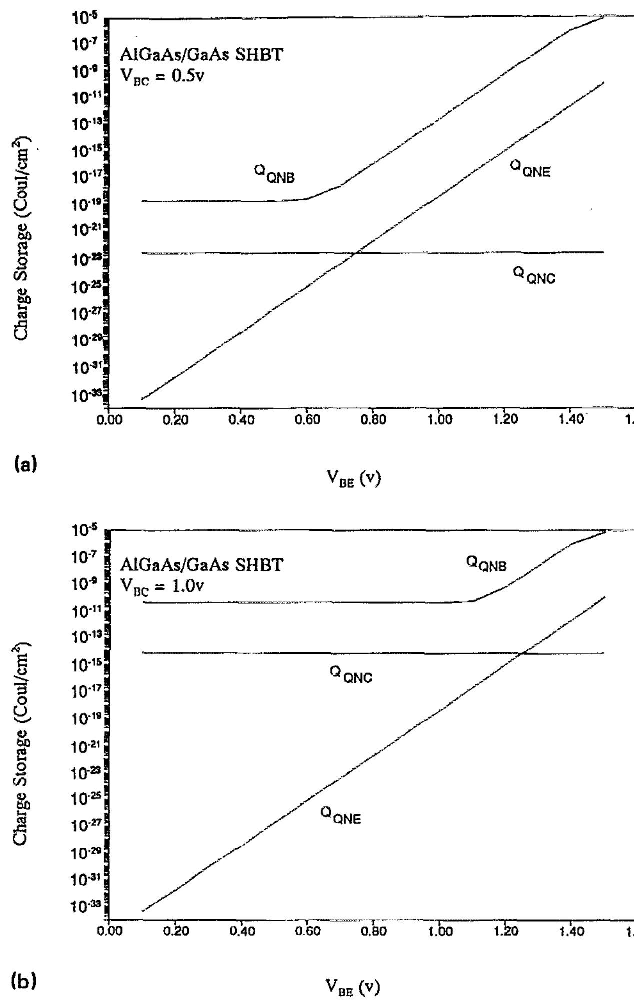

FIG. 5. Charge storage in the quasineutral emitter, base, and collector of the AlGaAs/GaAs/GaAs HBT for (a) $V_{BC}=0.5$ V; and (b) $V_{BC}=1.0$ V.

IV. RESULTS AND DISCUSSION

Using the device parameters given in Table I, we have calculated the minority-carrier charges stored in the quasineutral regions as well as the diffusion capacitances associated with this charge storage. Figures 4(a)–4(b) plot Q_{QNE}, Q_{QNB}, and Q_{QNC} vs V_{BE} for two different V_{BC} for the homojunction BJT. The change of slope from 1.0 to 0.5 for Q_{QNB} and Q_{QNE} results from high-level injection. Figures 5(a)–5(b) and 6(a)–6(b) show Q_{QNE}, Q_{QNB}, and Q_{QNC} vs V_{BE} for two different V_{BC} for the AlGaAs/GaAs SHBT and the Si/SiGe DHBT, respectively. The emitter-base and base-collector diffusion capacitances associated with these charges for the three transistors are given Figs. 7 and 8, respectively. Our calculations suggest that the Si BJT has a comparable C_{DE} as the Si/SiGe DHBT, but has a C_{DC} that is about an order larger than that in the Si/SiGe DHBT. The smaller C_{DC} in the Si/SiGe DHBT stems from the valence band discontinuity at the base-collector heteroface, which eliminates the injection of holes from the base into the collector and thus reduces the charge stored in the quasineutral collector. It is further shown that the AlGaAs/GaAs SHBT possesses much smaller C_{DE} and C_{DC} than Si BJT and Si/SiGe DHBT at a given bias condition. This advantage is primarily due to the fact that AlGaAs and GaAs have a larger energy band gap than Si and SiGe, which results in a smaller minority free-carrier concentration in the quasineutral regions under the same bias conditions.

We now examine the effects of the quasineutral-region charge storage on the cutoff frequency f_T of the transistor operated under forward-active mode. The cutoff frequency is given by[11]

$$f_T = 1/[2\pi(\tau_E + \tau_C + \tau_{CT} + \tau_{BT})], \quad (34)$$

where τ_E, τ_C, τ_{CT}, and τ_{BT} are the emitter capacitance charging time, the collector capacitance charging time, the collector junction transit time, and the base transit time, respectively. Since the base-collector junction is reverse biased and C_{DC} are negligibly small under forward-active operation, only τ_E will be affected by the charge stored in the quasineutral regions, which can be expressed as[11]

$$\tau_E = r_e A(C_{jE} + C_{DE}) \approx (4V_T/J_C)(C_{jE} + C_{DE}), \quad (35)$$

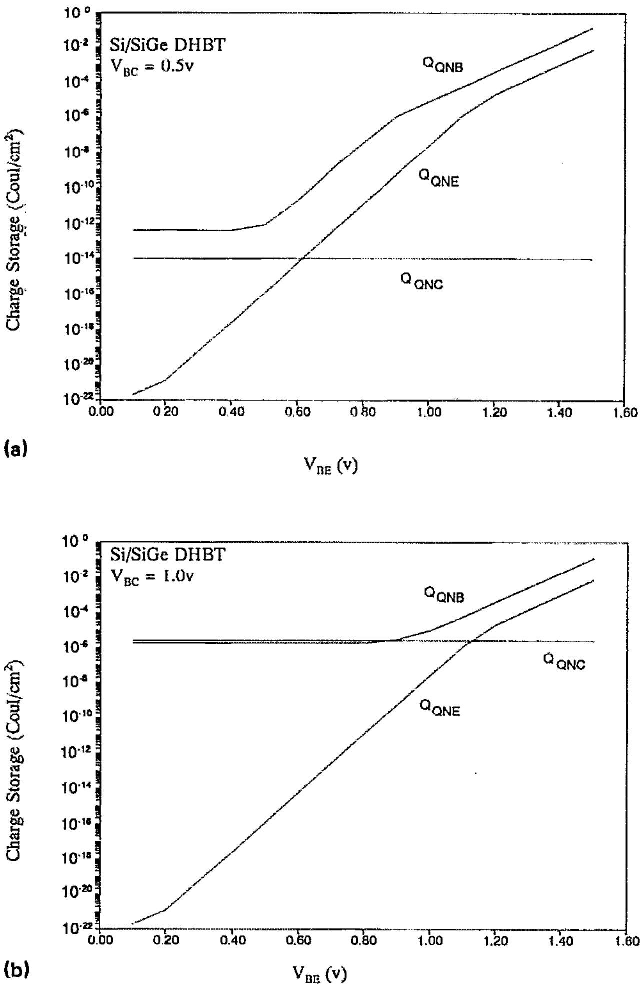

FIG. 6. Charge storage in the quasineutral emitter, base, and collector of the Si/SiGe/Si HBT for (a) $V_{BC}=0.5$ V; and (b) $V_{BC}=1.0$ V.

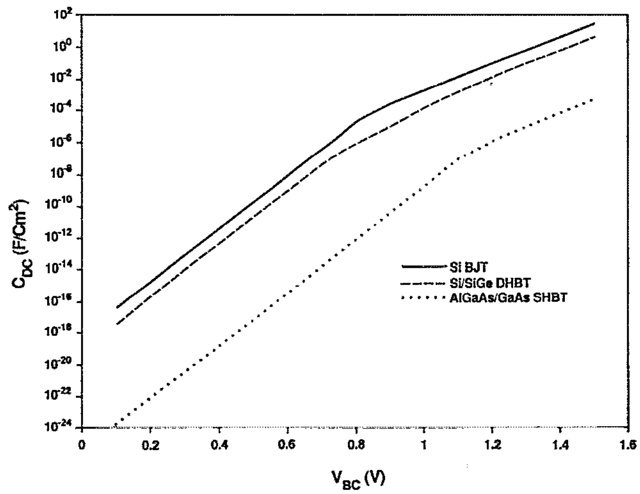

FIG. 8. Base-collector diffusion capacitances vs V_{BC} for the Si BJT, AlGaAs/GaAs SHBT, and Si/SiGe DHBT.

where r_e is the emitter-base junction resistance, A is the junction area, and C_{jE} is the emitter-base junction capacitance

$$C_{jE}=\{qN_EN_B\epsilon_E\epsilon_B/[2(\epsilon_EN_E+\epsilon_BN_B)(V_{bi,EB} - V_{j,BE})]\}^{0.5}. \tag{36}$$

Here ϵ_E and ϵ_B are the dielectric permittivity in the emitter and in the base, respectively. Note that for a Si homojunction BJT, $\epsilon_E=\epsilon_B=\epsilon_{si}$ and $C_{jE}=\{qN_EN_B\epsilon_{si}/[2(N_E+N_B)(V_{bi,EB}-V_{j,BE})]\}^{0.5}$. Figure 9 plots τ_E as a function of the collector current density J_C for the Si BJT, AlGaAs/GaAs SHBT, and Si/SiGe DHBT. At $J_C=10^6$ A/cm^2, which is the collector current density most bipolar transistors are designed to operate, τ_E in the AlGaAs/GaAs SHBT is about an order smaller than that in the Si/SiGe DHBT and is about two orders smaller than that in the Si BJT. Consequently, the AlGaAs/GaAs HBT

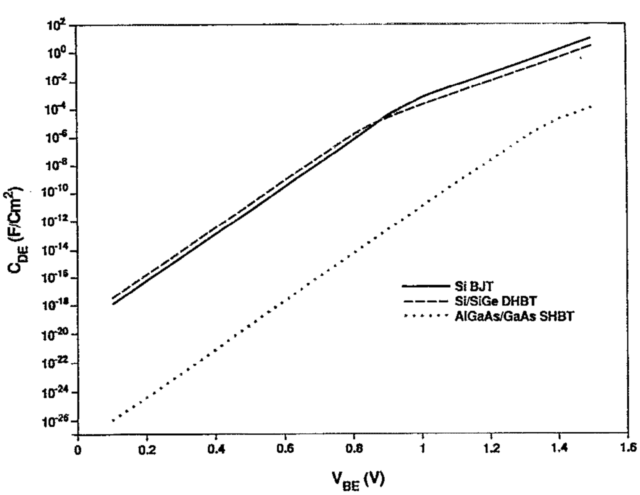

FIG. 7. Emitter-base diffusion capacitances vs V_{BE} for the Si BJT, AlGaAs/GaAs SHBT, and Si/SiGe SHBT.

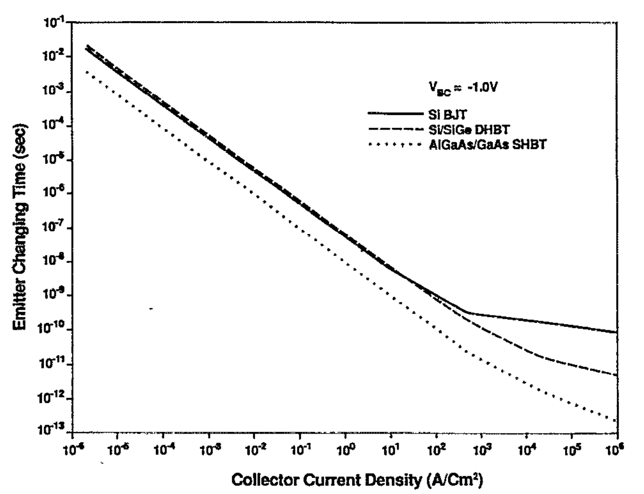

FIG. 9. Comparison of the emitter charging times for the Si BJT, AlGaAs/GaAs SHBT, and Si/SiGe DHBT calculated as a function of the collector current density.

should possess the highest cutoff frequency if τ_E is the limiting factor for f_T.

V. CONCLUSIONS

In summary, we have found that the minority free-carrier storage in the quasineutral regions of the AlGaAs/GaAs HBT is much smaller than that of the Si BJT and Si/SiGe HBT for a given applied voltage. This, together with the high electron mobility in GaAs-related materials, leads to the conclusion that the AlGaAs/GaAs HBT should have the fastest switching speed among the three transistors and that the AlGaAs/GaAs HBT should be used if speed is the primary concern. We further show that the Si/SiGe HBT has a comparable emitter-base diffusion capacitance, but has a smaller base-collector diffusion capacitance compared to the Si BJT. The reduction of the base-collector diffusion capacitance in the Si/SiGe HBT results from the valence band discontinuity at the base-collector heteroface, which reduces the minority-carrier injection from the base into the collector. As a result, the Si/SiGe HBT is expected to operate at a higher speed than its Si homojunction counterpart.

ACKNOWLEDGMENT

This work was supported in part by the UCF/DSR research Grant No. 16-22-923.

[1] P. M. Asbeck, M. F. Chang, J. A. Higgins, N. H. Sheng, G. J. Sullivan, and K. C. Wang, IEEE Trans. Electron Devices **36**, 2032 (1989).

[2] S. S. Iyer, G. L. Patton, J. M. C. Strok, B. S. Meyerson, and D. L. Harame, IEEE Trans. Electron Devices **36**, 2043 (1989).

[3] C. A. King, J. L. Hoyt, and J. F. Gibbons, IEEE Trans. Electron Devices **36**, 2093 (1989).

[4] I. E. Getreu, *Modeling the Bipolar Transistor* (Elsevier, New York, 1978).

[5] S. C. Jain and D. J. Roulston, Solid State Electron. **34**, 453 (1991).

[6] J. J. Liou, J. Appl. Phys. **66**, 286 (1989).

[7] E. S. Yang, *Microelectronic Devices* (McGraw–Hill, New York, 1988).

[8] J. J. Liou, Int. J. Electron. **72**, 89 (1992).

[9] M. Ugajin and Y. Amemiya, Solid State Electron. **34**, 593 (1991).

[10] H. Unlu and A. Nussbaum, IEEE Trans. Electron Devices **ED-33**, 616 (1985).

[11] M. Shur, *Physics of Semiconductor Devices* (Prentice–Hall, Englewood Cliffs, NJ, 1990).